THERMAL PERFORMANCE OF GREEN FAÇADES USING A NUMERICAL EVALUATION

Diogo Miguel Matias Cabrita Serpa

Thesis to obtain the Master of Science Degree in

Civil Engineering

Supervisors: Professor Maria Cristina de Oliveira Matos Silva
Professor Maria da Glória de Almeida Gomes

Examination Committee

Chairperson: Professor João Pedro Ramôa Ribeiro Correia
Supervisor: Professor Maria Cristina de Oliveira Matos Silva
Member of the Committee: Professor Daniel Aelenei

May 2016

1. Introduction

This paper is divided into seven chapters. The first chapter includes the initial considerations of green façades theme, while the second focuses on explaining the different types of green façades, the advantages and disadvantages, legislation and incentives for green façades construction and also some conclusions of other experimental studies. The third part includes the description of the two experimental cases, the first named Travessa do Patrocínio and the second Atlântico Blue Studio, located in Lisbon and Paço de Arcos. The fourth chapter summarizes the mathematical models of Susorova et al. (2013) and Malys et al. (2014) used to validate the experimental data collected by Prazeres (2015). The fifth chapter emphases the calculation of the heat transfer coefficient using three different methods. In sixth part is where the calibration occurs using the two mathematical models and in the last chapter of this document is presented the conclusions and some ideas for future investigations.

The growing concern with the environmental health of our cities occupy a prominent place in the world and comes with a relentless search for new solutions to minimize these problems. The urban sprawl, intensified use and land occupation, followed by strictly economic criteria, it causes shortage of urban land and the lack of green spaces. The appearance of green facades comes to help reducing these problems and to solve the lack of green spaces and vegetation on city streets. In this way we can improve the quality of the urban environment as well as creating new and innovative types of verticality. The use of this type of facade constructive solution is barely new in Portugal, where there is no legislation for structuring, still insufficient investigation of the quality / price, few companies who actually do it and few information available about the concept.

2. State of art

The origin of the green facade concept refers to the Hanging Gardens of Babylon, in 600 BC, one of the seven wonders of the ancient world to which its location remains yet unknown Woollaston (2013). Since the 80's, the concern about the environmental issues appeared, which resulted in the vision of bringing nature into the cities. Since then, further studies were performed on the effects of plants on facades such as isolation, the ability to mitigate dust, the cooling provided by plants, among other things, (Köhler, 2008).

2.1 Different types of green façades

Green facades are divided into two distinct types, the DGF (Direct Green Façade) and the LW (Living Wall). The DGF consists of placing plants like ivies to cover structures with their roots located on the floor, in intermediate space (vessels) or even on roofs. The reason for using plants like these relates to the fact that it allows them to attach directly to the wall. However, their growth can damage the wall or causing difficulties in maintenance or in plant replacement. The LW are more complex than the first , but more effective , since the plants must have certain properties in order to survive in the absence of substrate. They are composed of prefabricated panels, vertical modules or layers, which are fixed vertically on the structural wall. These panels can be of many different types of material support and can contain a wide variety of plant species. At which nutrients and water are supplied through an artificial system of fertirrigation/irrigation dropper Cameron et al. (2014) and Eumorfopoulou et al. (2010).

2.2. Green façade advantages/disadvantages

Green facades can help mitigate the loss of biodiversity caused by the effect of urbanization. It sustains a variety of plants, increases the production of oxygen and food, afford habitat and nesting places for several birds' species, Ottelé et al. (2011). Vegetation plays a key role in mitigating the effect of Heat Island Effect (HIE), managing to diminish the building absorbed radiation, leading to a local moisture growth due to plants evapotranspiration and consequent decrease in temperature, Sheweka et al. (2012). The presence of vegetation also decreases the building needs of air conditioners for cooling and heating, Ismail (2013). The economic effects have been investigated, particularly in green roofs, but it might have the same positive impact as green facades. According to Peck et al. (1999), it was

assumed that the building value increases about 6% to 15% while in presence of a green façade. In Perini et al. (2013) investigations, it was suggested that vegetation on facades and roads can increase land price by 1.4% in Tokyo and 2.7% in Kitakyushu.

2.3 Legislation and incentive for green façades construction

In Portugal there is still no regulation and incentive programs for green façades construction. However, in the last twenty years, some international cities have adopted economic incentives in order to support a wider green development in urban spaces. In most cases, these incentives are only related to green roofs and not to green facades, Perini et al. (2013). In the investigation of Scherer et al. (2013), it mentioned that was engendered incentives for green facades construction for cities like London and Toronto. In New York City, was created an economic incentive to reduce the green facades tax from 1.5$/m^2 to 3$/m^2, depending on its characteristics and on public benefits of it, Open (2014). In Germany cities, there are already incentive programs for green buildings, including green facades, Costa (2011).

2.4 Existing studies

There are a few studies that explore the green façades behavior and the way how they influence the building thermal performance. In the document of Eumorfopoulou et al. (2009) it was showed that the exterior surface temperature behind the vegetation can be reduced by 1.9°C to 8,3°C , depending on the foliage density. According to Wong et al. (2010), it was verified an air temperature reduction of 3.3°C, in which corresponded to a decrease in the surface temperature behind the vegetation by 1.1°C to 11.58°C, while in Holm (1989), the surface temperature behind the vegetation was reduced by 2.6°C. In Perini et al. (2011), it was concluded that the surface temperature behind the vegetation can be reduced by 1.2°C to 3.9°C. In Alexandri et al. (2008) was experienced a slighter effect on decreasing the surrounding temperature when the canyon between buildings was bigger. In Köhler et al. (1987), it was confirmed that a green façade surface temperature was 2°C to 6°C lower than a bare façade, although in Perez et al. (2011) the difference was 5,5°C. In Wong et al. (2010) was determined the heat transfer coefficient (U) of 0,365W/(m^2.°C) for a green roof and 3,344W/(m^2.°C) for a roof without vegetation. In green façades shouldn't be less different, however the thermal resistance of soil can affect U values significantly.

3. Case studies

The first case of study is a single-family building in Lisbon, named Travessa do Patrocínio. The vertical front covers 100 square meters and it is independent of the building, filled with 4500 plants of 25 different species and the construction is entirely traditional, made of concrete, Figure (1). The second case of study is a music studio located in Paco de Arcos, named Atlântico Blue Studio. The vertical green facade occupies 20 square meters and the green roof 28.5 square meters, Figure (2). The builder of these two green façades is the same, named ADN Design, so the layers of it are the same aswell.

Figure 1: Green Façade, Travessa do Patrocínio

Figure 2: Atlântico Blue Studio, Paço de Arcos

3.1 Case study: Travessa do Patrocínio

The green facade in Lisbon was monitored in two experimental campaigns in 2014, in winter from 21th to 27th February and 3rd to 10th March, and also in summer from 17th to 24th June and 3rd to 7th of July. The simulated area in bare façade of level 0 (office) it is presented as nrº7 (zone 1) and in green façade of level 2 (dining room) it is displayed as nrº 3 (vegetation), Figure (3).

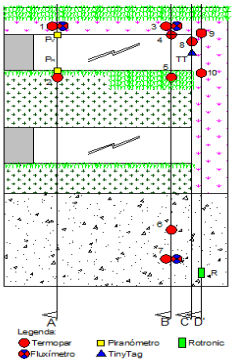

Figure 3: Representation of sensor positions in Travessa do Patrocínio by Prazeres (2015)

The office wall of level 0 is made of plaster, concrete, rockwool and two layers of plasterboard as shown in Figure(4) and the wall of the level 2 contains, vegetation, two layers of geotextile with a pipe between, PVC, air box, projected polyurethane, concrete, air box and two layers of plasterboard, presented in Figure(5).

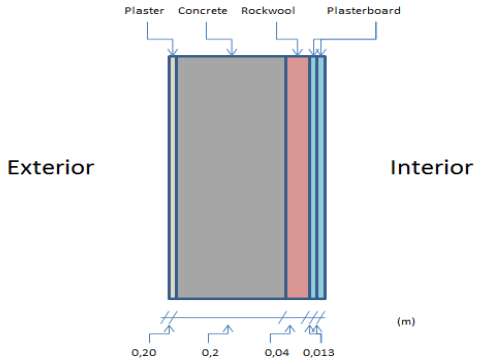

Figure 4: Office wall layers of Level 0, Travessa do Patrocínio

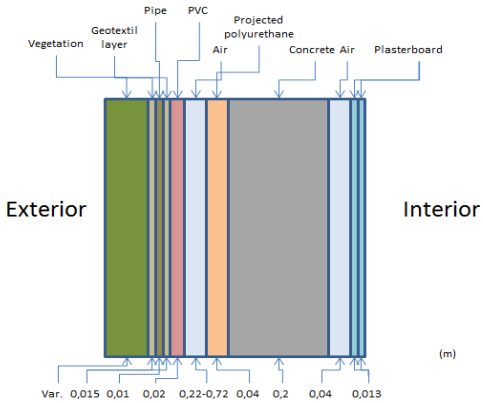

Figure 5: Living room wall layers of Level 2, Travessa do Patrocínio

3.2 Case study: Atlântico Blue Studio

The green façade monitoring in Paço de Arcos was held in two experimental campaigns conducted in 2014. The first was in winter, 13th to 19th February and 27th February to 13th March, and another held in summer, from June 18th to July 2nd and 5th to 10th July. The simulated area in green roof it is displayed as nrº1 and in green façade are presented as nrº2 (zone 1) and as nrº4 (zone 2), Figure(6).

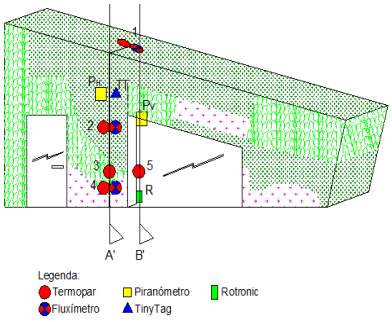

Figure 6: Representation of sensor positions in Atlântico Blue Studio by Prazeres (2015)

The green facade wall is made of vegetation, two layers of geotextile with a pipe between, geotextile layers, PVC, air box, and it was assumed that the rest would be made of plaster, brick, air box, Figure (7). In the green roof there is, vegetation, two layers of geotextile with a pipe between, PVC, projected polyurethane, concrete, air box (false ceiling) and plasterboard. It has a slope of a 30 degrees, Figure (8).

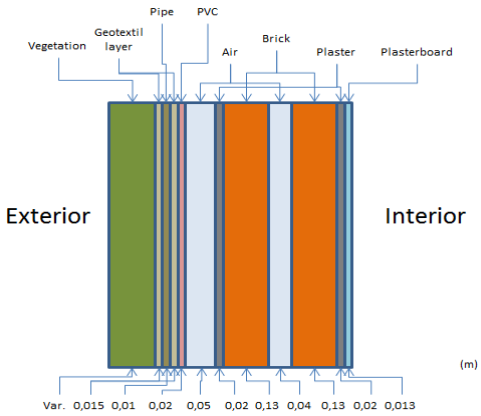

Figure 7: Green façade, Atlântico Blue Studio

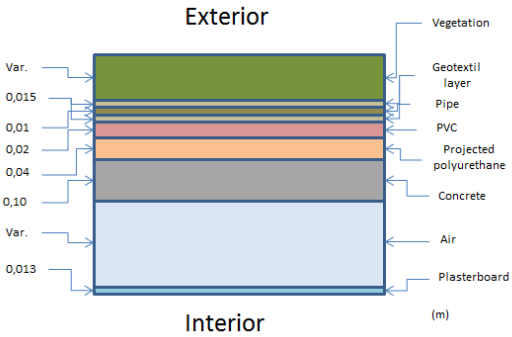

Figure 8: Green roof, Atlântico Blue Studio

4. Mathematical models

4.1 Susorova, et al. (2013) model

The mathematical model of Susorova et al. (2013) simulates the ability which plants have in facade thermal performance using parameters such as, facade properties, building orientation and weather conditions. It contains plants physiological processes such as evaporation, heat exchange by convection and radiation between the plants, facade, surrounding areas and ground. About the individual characteristics of plants, includes the absorptivity of the leaf, leaf size, leaf area index (*LAI*), radiation attenuation coefficient, stomatal conductance and resistance of the leaf. In this model, the energy balance of the bare façade (*psv*) equation (1) depends on shortwave radiation (SR_{psv}) W/m^2, long wave radiation (LR_{psv}) W/m^2, convection (C_{psv}) W/m^2, heat flux through the front wall (Q_{psv}) W/m^2 and the stored heat in the facade wall material (S_{psv}) W/m^2. The energy balance of the green façade (*pcv*), equation (2), has the same phenomena of the bare façade, but there is a radiation exchange between the wall and the vegetation ($LR_{pcv\text{-}f}$) W/m^2.

$$SR_{psv} + LR_{psv} + C_{psv} = Q_{psv} + S_{psv} \quad (1)$$

$$SR_{pcv} + LR_{pcv} + C_{pcv} + LR_{f-pcv} = Q_{pcv} + S_{pcv} \quad (2)$$

The short wave radiation in *psv*, equation (3) includes the total incident solar radiation on façade surface (I_t) and the wall absorptivity (α_{par}), while in the *pcv* includes also the radiation transmissivity coefficient (τ), equation (4).

$$SR_{psv} = I_t \alpha_{par} \quad (3)$$

$$SR_{pcv} = I_t \alpha_{par} \tau \quad (4)$$

τ depends indirectly of the radiation attenuation coefficient (*k*) and *LAI* (m^2/m^2). *K* is dimensionless and its value is between 0 and 1. This variability is due to leaf angle, like K = 0 when the leaf is perpendicular to the facade and K = 1 when it is parallel, equation (5). While *LAI* is also dimensionless but its value is between 0.01 and 7.

$$\tau = e^{(-K\,LAI)} \quad (5)$$

The long wave radiation in *psv*, equation (6) and *pcv*, equation (7) includes radiation from sky and ground, wall emissivity (ε_p), sky emissivity ($\varepsilon_{céu}$) and ground emissivity ($\varepsilon_{chão}$) are dimensionless, and the temperatures measured in degrees, like clear sky ($T_{céu}$), ground ($T_{chão}$), exterior bare façade surface ($T_{sext,pcv}$) and exterior green façade surface ($T_{sext,psv}$). The long wave radiation of sky and ground are presented in equation (8) and (9), respectively.

$$LR_{psv} = LR_{céu} + LR_{chão} \quad (6)$$

$$LR_{pcv} = \tau\, LR_{céu} + \tau\, LR_{chão} \quad (7)$$

$$LR_{céu} = \varepsilon_p\, \varepsilon_{céu}\, \sigma\, F_{céu} \left(T_{céu}^4 - T_{s\,ext,psv}^4\right) \quad (8)$$

$$LR_{chão} = \varepsilon_p\, \varepsilon_{chão}\, \sigma\, F_{chão} \left(T_{chão}^4 - T_{s\,ext,psv}^4\right) \quad (9)$$

$F_{céu}$ and $F_{chão}$ are view factors dependents on wall surface-ground angle (θ) in degrees, equation (10) and (11).

$$F_{chão} = 0.5\,(1 - cos\,\theta) \quad (10)$$

$$F_{céu} = 0.5\,(1 + cos\,\theta) \quad (11)$$

The temperature of clear sky ($T_{céu}$), equation (12), depends on exterior air temperature ($T_{air,ext}$) and dew point temperature (T_{orv}), equation (13). This parameter is derived from an empirical correlation made by Bulk (1981).

$$T_{céu} = T_{ar,ext}\,[0.8 + (T_{orv} - 273)/250]^{0.25} \quad (12)$$

$$T_{orv} = \frac{c\,\ln\left(\frac{HR}{100} e^{\left(\left(b - \frac{T_{ar,ext}}{d}\right)\left(\frac{T_{ar,ext}}{c + T_{ar,ext}}\right)\right)}\right)}{b - \ln\left(\frac{HR}{100} e^{\left(\left(b - \frac{T_{ar,ext}}{d}\right)\left(\frac{T_{ar,ext}}{c + T_{ar,ext}}\right)\right)}\right)} \quad (13)$$

b = 18.678; c = 257.14°C and d = 234.5°C

The convection in *psv* and *pcv* is described in the equations (14) and (15). The first equation includes the difference between exterior air temperature ($T_{ar,ext}$) and exterior bare façade temperature ($T_{sext,psv}$), while the second presents the difference between exterior air temperature ($T_{ar,ext}$) and exterior green façade surface temperature ($T_{sext,pcv}$).

$$C_{fsv} = h_{psv}(T_{ar,ext} - T_{s\,ext,psv}) \quad (14)$$

$$C_{fcv} = h_{pcv}(T_{ar,ext} - T_{s\,ext,fcv}) \quad (15)$$

The paramaters h_{psv} and h_{pcv} W/(m^2.°C) are the same due to the lack of information about wind speed ($V_{ar,ext}$) m/s, equation (16).

$$h_{psv} = h_{pcv} = 10.79 + 4.192\, V_{ar,ext} \quad (16)$$

The heat stored in wall material of bare façade (S_{psv}) and green façade (S_{pcv}) are dynamic and time dependent, equation (17) and (18).

$$S_{psv} = L\, c_{P,p}\, \rho_p \left(\frac{dT_{s\,ext,psv}}{dt}\right) \quad (17)$$

$$S_{pcv} = L\, c_{P,p}\, \rho_p \left(\frac{dT_{s\,ext,pcv}}{dt}\right) \quad (18)$$

The wall thickness (L) is in meters, while the wall specific heat ($C_{p,p}$) is measured in J/(kg.°C), the wall density material (ρ_p) in kg/m^3 and time variation (dt) in seconds. The total heat flow through the bare façade (Q_{psv}), equation (19) and green façade (Q_{pcv}), equation (20) includes the variation between the exterior and interior façade surface temperature and the wall thermal resistance (R).

$$Q_{psv} = \frac{T_{s\,ext,psv} - T_{s\,int,psv}}{R_{psv}} \quad (19)$$

$$Q_{pcv} = \frac{T_{s\,ext,pcv} - T_{s\,int,pcv}}{R_{pcv}} \quad (20)$$

The radiation exchange between leaf and green façade (LR_{f-pcv}) is characterized by wall and leaf emissivity, and also by the difference between exterior green façade surface temperature and leaf temperature, equation (21).

$$LR_{f-pcv} = (1-\tau)\frac{\varepsilon_p\, \varepsilon_f}{\varepsilon_p + \varepsilon_f - \varepsilon_p\, \varepsilon_f}\left(T^4_{s\,ext,pcv} - T^4_f\right) \quad (21)$$

The Leaf temperature is very complex because its calculation includes some physiological processes, equation (22).

$$T_f = T_{ar,ext} + \frac{Y'}{\frac{\Delta}{P_{ar}} + Y'}\left[\frac{Q_f}{g_c\, c_{p,ar}} - \frac{e_s(T) - e_a}{P_{ar}\, Y'}\right] \quad (22)$$

The apparent psychometric constant (Y'), equation (23), depends on the ratio between the heat conductance through the air (g_c), equation (24) and vapor conductance through the air (g_v), equation (25) in mol/(m^2.s).

$$Y' = \frac{Y\, g_c}{g_v} \quad (23)$$

$$g_c = g_{lcc} + g_r \quad (24)$$

$$g_v = \frac{0.5\, g_{ea\,ss}\, g_{lcv}}{g_{ea\,ss} + g_{lcv}} + \frac{0.5\, g_{ea\,si}\, g_{lcv}}{g_{ea\,si} + g_{lcv}} \quad (25)$$

Upper ($g_{ea\ ss}$) and lower ($g_{ea\ si}$) leaf surface stomatal conductance were obtained experimentally by Gates (2003). The boundary layer for vapor (g_{lcv}) is presented in equation (26) and the boundary layer conductance for heat transfer through air (g_{lcc}) is in equation (27), which are directly related to wind speed ($V_{ar,ext}$) and inversely with the plant height (D_f). The radiative conductance (g_r) displayed in equation (28) is obtained by Campbell (1998) tables and it is related to wall emissivity, Stefan-Boltzmann constant σ=5,67x10^{-8} W/(m^2.°C), exterior air temperature and air specific heat at constant pressure, $C_{p,ar}$=29.3 J/(mol.°C).

$$g_{lcv} = 1.4\left(0.147\sqrt{\frac{V_{ar,ext}}{D_f}}\right) \quad (26)$$

$$g_{lcc} = 1.4\left(0.135\sqrt{\frac{V_{ar,ext}}{D_f}}\right) \quad (27)$$

$$g_r = \frac{4\,\varepsilon_p \sigma\, T^3_{ar,ext}}{C_{p,ar}} \quad (28)$$

The total radiation absorbed by the leaf (Q_f), includes the radiation absorbed and the emitted radiation, equation(29).

$$Q_f = I_t \alpha_f + \varepsilon_f\, \sigma\, F\, (T^4_{céu} + T^4_{chão}) - \varepsilon_f\, \sigma\, (T_{ar,ext})^4 \quad (29)$$

The leaf absorptivity (αf) is dimensionless and represents the fraction of incident radiation absorbed by leaf surface. The water vapor pressure of air saturation $e_s(T_{ar,ext})$ is measured in kPa, equation(30) and the partial water vapor pressure of the air (e_a) is too in kPa, equation(31). These parameters are directly proportional to the air temperature and air humidity.

$$e_s(T_{ar,ext}) = 0{,}611\, e^{\left(\frac{17.502\, T_{ar,ext}}{T_{ar,ext} + 240.97}\right)} \quad (30)$$

$$e_a = e_s(T_{ar,ext})Hr \quad (31)$$

The slope of the saturation vapor pressure (Δ) in kPa/°C is given by equation(32).

$$\Delta = \frac{4217 e_s(T_{ar,ext})}{(240.97 + T_{ar,ext})^2} \quad (32)$$

In the model of Susorova et al. (2013), considered the outer surface temperature as output. To this end, it was necessary to properly establish the input climatic conditions, such as wind speed , relative humidity of the air outside the incident solar radiation on the facade and the outer air temperature; Façade conditions such as the inner façade surface temperature, the heat transfer coefficient , emissivity wall, the absorptance, the density, the specific heat and the wall density; Plant characteristics such as LAI, leaf dimension, stomatal conductance, attenuation radiation coefficient and leaf emissivity.

4.2 Malys et al. (2014) model

The mathematical model of Malys et al. (2014) simulates the Living Wall façade thermal performance considering the effect on leafs, air between leafs and wall. In figure (9)

there is presented a scheme of all physiological phenomenon occurring in this model. The three main equations which define the leaf, air between leafs and substrate thermal balance are equations(33), (34) and (35).

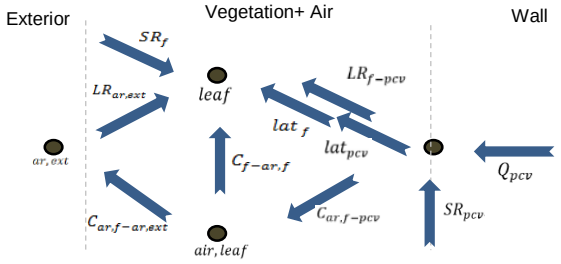

Figure 9: Scheme of physiological phenomenon occurring in this model

$$Co_f \frac{dT_f}{dt} = SR_f + LR_{ar,ext} + LR_{f-pcv} + C_{f-ar,f} + lat_f \quad (33)$$

$$Co_{ar,f} \frac{dT_{ar,f}}{dt} = -C_{f-ar,f} + C_{ar,f-pcv} + C_{ar,f-ar,ext} \quad (34)$$

$$Co_{fcv} \frac{dT_{fcv}}{dt} = SR_{pcv} - LR_{f-pcv} - C_{ar,f-pcv} + Q_{pcv} - lat_{pcv} \quad (35)$$

The terms Co_f presented in equation(36), $Co_{ar,f}$ in equation(37) and Co_{fcv} in equation (38) represent the leafs thermal capacitance, air between leafs and wall. These parameters are defined by thickness (D), density (ρ) and specific heat (c_p). According to leaf thermal capacitance, also includes *LAI*. These equations are similar to the heat stored in Wall material equations(15) and (16) from Susorova et al.(2013).

$$Co_f = d_f \, \rho_{ag} \, c_{p,ag} \, LAI \quad (36)$$

$$Co_{ar,f} = D_{ar,f} \, \rho_{ar} c_{p,ar} \quad (37)$$

$$Co_{pcv} = D_p \, \rho_p \, c_{p,p} \quad (38)$$

The short wave radiation on leaf (SR_f), equation(39) includes total short-wave solar radiation (I_t) in W/m², the radiation transmissivity coefficient (τ) and leaf albedo (A_f). The short wave radiation on wall (SR_{pcv}) doesn't include leaf albedo, equation(40).

$$SR_f = (1 - \tau - A_f) I_t \quad (39)$$

$$SR_{pcv} = \tau \, I_t \quad (40)$$

The long wave radiation is characterized by heat-radiation flow from the atmosphere and radiation exchanges coming from multiple surfaces ($LR_{ar,ext}$), equation(41) and radiation exchange between leaf and exterior substrate surface ($LR_{f,pcv}$), equation(42).

$$LR_{ar,ext} = F_{céu}(I_{ir} - \sigma T_f^4) + \sigma \sum \left(F_i(\varepsilon_i T_i^4 - \varepsilon_f T_f^4)\right) \quad (41)$$

$$LR_{f-pcv} = h_{f-pcv}(T_f - T_{pcv}) \quad (42)$$

The solar radiation longwave from the atmosphere (I_{ir}) is measured in W/m², the radiation heat transfer by between exterior substract surface an leaf ($h_{f\text{-}pcv}$) is presented in equation(43), the convective heat transfer coefficient in air ($h_{ar,f\text{-}ar,ext}$) in displayed in equation(44), the convective heat transfer coefficient at leaf surface ($h_{f\text{-}ar,f}$) is exhibited in equation(45) and the convective heat transfer coefficient at substract surface ($h_{ar,f\text{-}pcv}$) is showed in equation(46). This last parameter was assumed to be equal as $h_{f\text{-}pcv}$.

$$h_{f-pcv} = h_{ar,f-pcv} = 4 \, \sigma \, T_f^3 \quad (43)$$

$$h_{ar,f-ar,ext} = R(v) \, Co_{ar,f} \quad (44)$$

$$h_{f-ar,f} = 2 \, LAI \left(\frac{\rho_{ar} C_{p\,ar}}{R_{aero}}\right) \quad (45)$$

The air exchange rate in canopy (*R*) depends on wind speed ($V_{ar,ext}$), on weighting coefficient of wind speed for the air exchange rate (α_R) and on leaf aerodynamic resistance (R_{aero}). It is measured in s^{-1} and it is showed in equation(46).

$$R = R_{máx} + \alpha_R \frac{V_{ar,ext}}{V_{ar,ext\,máx}} (R_{máx} - R_{mín}) \quad (46)$$

The convection is characterized by three equations, the first considers the relationship between leaf and air displayed in equation (47), the second contemplates the air between leafs and substract displayed in equation(48), the third one is about the exterior air and air between leafs, presented in equation(49). It includes leaf, air between leafs and substract temperatures and the convective heat transfer coefficients exhibited in equations (43), (44) and (45).

$$C_{f-ar,f} = h_{f-ar,f}(T_f - T_{ar,f}) \quad (47)$$

$$C_{ar,f-pcv} = h_{ar,f-fcv}(T_{pcv} - T_{ar,f}) \quad (48)$$

$$C_{ar,f-ar,ext} = -h_{ar,f-ar,ext}(T_{ar,f} - T_{ar,ext}) \quad (49)$$

The heat thermal flux through façade wall (Q_{pcv}) presented in equation(50) depends on temperature difference between exterior and interior surface, and wall thermal resistance (R).

$$Q_{pcv} = \frac{(T_{s.int} - T_{s.ext})}{R_{pcv}} \quad (50)$$

The latent thermal flux on leaves (lat_f) and on substract (lat_{pcv}) displayed in equations (51) and (52) are characterized by the repartition coefficient (α_{lat}),

representing the distribution between plant transpiration and water evaporation, evapotranspiration (ETP) and evapotranspiration rate (f). The ETP used in this model is related to Penman-Monteith equation, while *f* depends on water stress in substrate. In this model, *f* was considered equal to 1.

$$lat_f = \alpha_{lat} f\ ETP \quad (51)$$

$$lat_{pcv} = (1 - \alpha_{lat})\ f\ ETP \quad (52)$$

In Malys et al . (2014) model it was considered the outer surface temperature , leaf temperature and air between leafs and substract temperature as outputs . To this end, it was necessary to properly establish the input climatic conditions, such as wind speed, relative humidity, incident solar radiation on the facade and outer air temperature; Facade conditions such as inner surface facade temperature, heat transfer coefficient, wall emissivity and density , specific heat and width ; Plant characteristics such as LAI, leaf size, leaf albedo, leaf stomatal resistance, leaf thickness, aerodynamic resistance, attenuation of radiation coefficient and leaf emissivity.

5. Heat transfer coefficient

There were used three different formulas for heat transfer coefficient calculation, and they are: $U_{(i)}$ based on thermal resistance from different layers displayed in equation(53); $U_{(ii)}$ progressive average based on exterior and interior temperatures presented in equation(54) and $U_{(iii)}$ progressive average based on surfaces temperatures exhibited in equation(55).

$$U_{(i)} = \frac{1}{\left(R_{si} + R_{se} + \sum R_j\right)} \quad (53)$$

$$U_{(ii)} = \frac{\sum_o^{i-t} Q_i}{\sum_o^{i-t} Tint_i - \sum_o^{i-t} Text_i} \quad (54)$$

$$U_{(iii)} = \frac{1}{\frac{\sum_0^{i-t} Ts,int_i - \sum_0^{i-t} Ts,ext_i}{\sum_0^{i-t} Qi} + R_{se} + R_{si}} \quad (55)$$

In Tables (1) and (2) are displayed the heat transfer coefficients used for models validation in both study cases. Notice that the $U_{(ii)}$ results aren't showed in those tables since the calculations of $U_{(iii)}$ are closer to the real coefficient.

Table 1 – Heat transfer coefficient, $U_{(i)}$ and $U_{(iii)}$, winter and summer, Travessa do Patrocínio

	Heat transfer coefficient (U), W/(m².°C)			
	PISO 2		PISO 0	
Season	$U_{(i)}$	$U_{(iii)}$	$U_{(i)}$	$U_{(iii)}$
Winter	0,362	2,224	0,720	-
Summer				

Table 2 – Heat transfer coefficient, $U_{(i)}$ and $U_{(iii)}$, winter and summer, Atlântico Blue Studio

	Heat transfer coefficient (U), W/(m².°C)					
	Green Roof		Green Façade			
			Zone 1		Zone 2	
Season	$U_{(i)}$	$U_{(iii)}$	$U_{(i)}$	$U_{(iii)}$	$U_{(i)}$	$U_{(iii)}$
Winter	0,426	1,251	0,519	1,833	0,493	1,424
Summer	0,413	1,640		1,836		1,263

In Travessa do Patrocínio for 2nd level were detected significant differences in heat transfer coefficients between $U_{(i)}$ and the rest. The experimental period in which there was a better approach of $U_{(ii)}$ and $U_{(iii)}$ in 2nd floor was between 21 to 27 February. In ground level, that approach did not happen. Also in February, the calculation of U through $U_{(iii)}$ converged to $U_{(i)}$ for ground level . In the case of Atlantic Blue Studio, the results of $U_{(i)}$ diverged significantly from other calculations because took into consideration the thermal resistance of all the materials involved in the process, while the values of $U_{(ii)}$ and $U_{(iii)}$ had in account the experimental data collected by Prazeres(2015) .

6. Calibration

The calibration intends to evaluate the outer surface temperature calculated by the two models with which it was gathered experimentally by Prazeres(2015). The solar radiation required as an input for models development was determined from the interaction of three programs, Sketchup (2013), EnergyPlus (2013) and OpenStudio (2013) using the equation (56).

$$Rd.dir.nor = \frac{Rd.glob.hor.\ (METEO) - Rd.dif.hor.(Eplus)}{\sin(a)} \quad (56)$$

In order to evaluate the difference between experimental and simulated data, it was use two parameters, RMSE, equation(57) and Pearson correlation coefficient (r), equation(58).

$$RMSE = \sqrt{\frac{\sum_{i=1}^{n}\left(X_{obs,i} - X_{modelo,i}\right)^2}{n}} \quad (57)$$

$$r = \frac{\sum_{i=1}^{n}\left[(x_i - \bar{x}) \times (y_i - \bar{y})\right]}{\sqrt{\sum_{i=1}^{n}(x_i - \bar{x})^2 \times \sum_{i=1}^{n}(y_i - \bar{y})^2}} \quad (58)$$

6.1 Travessa do Patrocínio

6.1.1 Susorova et al. (2013) model

The first point to be validated focused on the leaf temperature, equation (3.27), comparing with the study Gates (2003) and the Susorova et al. (2013), the differences between the values. This comparison aimed to clarify that the calculation of leaf temperature for model calibration in the both studies didn't oscillate more than > 1°C from Susorova et al. (2013) and Gates (2003) calculations. In Table (3) are displayed those results.

Table 3 – Differences of leaf temperatures between present study and Susorova et al. (2013) and Gates (2003)

Radiation absorbed (W/m²)	Susorova et al. (2013)			Gates (2003)		
	Leaf temperature (°C)			Leaf temperature (°C)		
	0,1 (m/s)	1 (m/s)	5 (m/s)	0,1 (m/s)	1 (m/s)	5 (m/s)
419	-0,92	-0,7	-0,52	-0,06	-0,38	-0,63
698	-0,04	-0,13	-0,11	-0,07	-0,05	-0,1
977	0,84	0,44	0,27	-0,08	-0,28	-0,37

For Susorova et al. (2013) model was assumed that for the beginning of the simulation, the temperature of the outer surface would be the same as the experimental surface outside temperature, and leaf temperature would be equal to the outdoor air temperature. The calibration of this model had constant parameters but some had changed during the experimental data collection. In Tables (4) and (5) are displayed general and plant data in Travessa do Patrocínio that kept unchanged during the simulation.

Table 4 – General Data, Travessa do Patrocínio

	Parameters			
General Data	γ (1/°C)	0,000666	$\varepsilon_{céu}$	1
	$F_{céu}=F_{chão}$	0,5	ε_{reboco}	0,87
	P_{ar} (kPa)	100	$\varepsilon_{chão}$	0,9
	$C_{p\ ar}$ J/(kg.°**C**)	1005	σ	5,67E-08
	$C_{p\ água}$ J/(kg.°**C**)	4187	$\rho_{água}$ (kg/m³)	1000
	$\alpha_r = \alpha_{lat}$	0,5	ρ_{ar} (kg/m³)	1,29

Table 5 – Plant Data, Travessa do Patrocínio

	Parameters			
Plants Data	ε_{folha}	0,96	K	0,4
	α_{folha}	0,5	Af	0,25
	df (m)	0,00015	R_{aero} (s/m)	50
	k	0,41	K	0,4

In Table (6) it is showed *LAI* and plant dimension in winter and summer for Travessa do Patrocínio

Table 6 – Different Plant Data in summer and winter, Travessa do Patrocínio

		Parameters		
		LAI (m²/m²)	D_f (m)	τ
Level 2	**Winter**	1	0,1	0,67
	Summer	1,8	0,1	0,49

Travessa do Patrocínio have multiple materials, so it was necessary to standardize wall material density and specific heat, equations (59) and (60).

$$\rho_{par} = \frac{\rho_{mat,1} \times e_{mat,1} + \cdots + \rho_{mat,n} \times e_{mat,n}}{e_{total}} \quad (59)$$

$$c_{P,par} = \frac{c_{P,mat\ 1} \times e_{mat,1} + \cdots + c_{P,mat\ n} \times e_{mat,n}}{e_{total}} \quad (60)$$

These values are displayed in Table (7) for level 0 and 2.

Table 7 – Wall density and specific heat, Travessa do Patrocínio

		$c_{P,parede}$ J/(kg.°C)	ρ_{parede} kg/m³
Level 0		864,06	1763,81
Level 2	**Bare façade**	911,76	1546,42
	Green façade	991,92	618,05

In Table (8) is presented the RMSE and correlation parameters of outer surface temperature for Level 0 and Level 2 in Travessa do Patrocínio according to the calculations of heat transfer coefficient through $U_{(iii)}$ of Chapter (5).

Table 8 – RMSE and *r* for Level 0 and 2, Travessa do Patrocínio

	21st to 27th February		3rd to 10th March		17th to 24th June		3rd to 7th July	
	RMSE	Corre. (0-1)	RMSE	Corre. (0-1)	RMSE	Corre. (0-1)	RMSE	Corre. (0-1)
$T_{s.ext\ Level\ 0}$ (°C)	3,988	0,858	4,098	0,637	1,897	0,807	2,652	0,813
$T_{s.ext\ Level\ 2}$ (°C)	2,945	0,693	3,737	0,738	2,959	0,526	3,559	0,487

RMSE values are closer to 4 ° C for the months of February and March, while in June and July, the error assumes slightly lower values. There are lower correlations between experimental and simulated data for Level 2 but higher correlations for level 0. In Figure (10) is displayed the comparison between simulation and measured data collected by Prazeres (2015) for Level 2 in June in Travessa do Patrocínio.

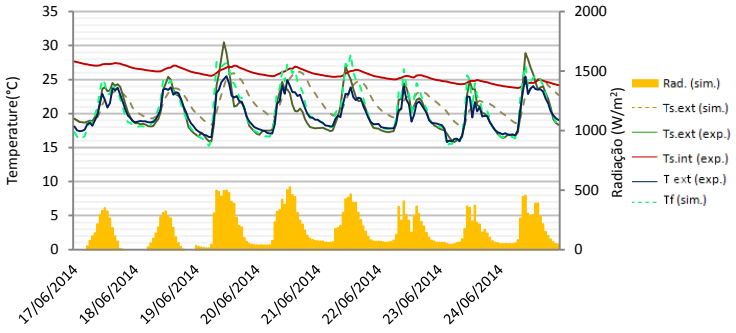

6.1.1 Malys et al. (2014) model

The first aspect to be analyzed focused on the latent heat flux because it is a complex parameter which depends on evapotranspiration (ETP) Penman- Monteith. The calculated latent heat flow was compared with the one used in in Malys et al. (2014) model in order to verify the same behavior.

The validation of this model had constant parameters while others have changed during the experimental data collection. In Table (9) is displayed general and plants data in Atlântico Blue Studio that kept unchanged during the simulation. In Malys et al. (2014) model calibration it was used the same values of specific heat, wall density, and also the plant parameters, LAI and plant size of Susorova et al. (2013) model.

In Table (10) is presented the RMSE and correlation parameters of outer surface temperature for Level 2 in Atlântico Blue Studio according to the calculations of heat transfer coefficient $U_{(iii)}$ of Chapter (5).

Table 9 – General and Plants Data, Atlântico Blue Studio

	Parameters					
General Data	γ (1/°C)	0,000666	$\varepsilon_{céu}$	1	α r	0,5
	$F_{céu} = F_{chão}$	0,5	$\varepsilon_{chão}$	0,7	σ	5,67E-08
	ρ_a(kg/m³)	1,29	ρ água (kg/m³)	1000	α lat	0,5
	$C_{p\ ar}$ J/(kg.ºC)	1005	$C_{p\ água}$ J/(kg·ºC)	4187		
Plants	ε_{folha}	0,96	K	0,4	k	0,41
	α_{folha}	0,5	Af	0,25		
	df (m)	0,00015	R_{aero} (s/m)	50		

Table 10 – RMSE and *r* for Level 2, Atlântico Blue Studio

	21st to 27th of February		3rd to 10th March		17th to 24th June		3rd to 7th July	
	RMSE	*Corre. (0-1)*	*RMSE*	*Corre. (0-1)*	*RMSE*	*Corre. (0-1)*	*RMSE*	*Corre. (0-1)*
$T_{s.ext\ Level\ 2}$ (°C)	2,897	0,640	2,414	0,731	1,751	0,830	1,904	0,794

RMSE has values close to 3°C values for February and March, while in June and July, the error takes values close to 2°C. There are better correlation values for summer campaign, althought for both seasons the correlation is higher than 0,5. In Figure (11) is displayed the comparison between simulation and measured data collected by Prazeres (2015) for Level 2 in June for Atlântico Blue Studio. The level 2 façade outer surface temperature comparison between Susorova et al. (2013), Malys et al. (2014) and the experimental collected by Prazares (2015) is displayed in Figure (12).

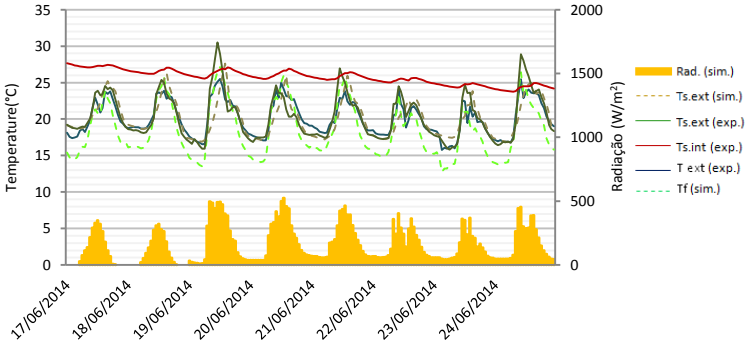

Figure 11: Comparison between simulation and measured data collected by Prazeres (2015), June, green façade, Travessa do Patrocínio

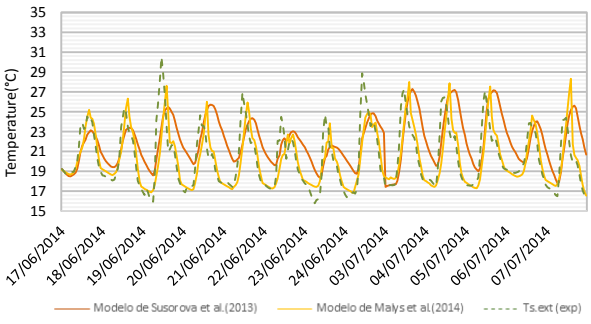

Figure 12: Comparison between simulation and measured data collected by Prazeres (2015), June, green façade, Travessa do Patrocínio

It was concluded that the outer surface temperature in Malys et al. (2014) model approached better to the experimental data. Notice that after the maximum daily peak, the temperature of the outer surface through the model Susorova et al. (2013) takes longer to cool than Malys et al. (2014).

6.2 Atlântico Blue Studio

6.2.1 Susorova et al. (2013) model

The model simulation parameters presented in Tables (4) and (5) were used for Atlantic Blue Studio study case, but floor emissivity (εchão) was different. The reason for this is due to the different ground material, wood (0.87). The air-box width in rooftop assumed 0.3m for the heat transfer coefficient calculation. The LAI and plant dimension have changed between winter and summer and these is showed in Table (11).

Table 11 – Different Plant Data in summer and winter, Atlântico Blue Studio

		Parameters		
		LAI (m^2/m^2)	D_f (m)	τ
Zone 1	Winter	1	0,1	0,67
	Summer	1	0,1	0,67
Zone 2	Winter	1,8	0,2	0,49
	Summer	1,8	0,2	0,49
Roof	Winter	1	0,1	0,67
	Summer	1	0,1	0,67

The specific heat and wall density are displayed in Table (12).

Table 12 – Wall density and specific heat, Atlântico Blue Studio

	$c_{P,parede}$ J/(kg.ºC)	ρ_{parede} kg/m³
Zone 1	1032,7	1000,0
Zone 2	1032,7	1000,0
Roof	1010,1	603,4

In Table (13) is presented the RMSE and correlation parameters of outer surface temperature for Zone 1 and 2, and also for green roof in Atlântico Blue Studio according to the calculations of heat transfer coefficient $U_{(iii)}$ of Chapter (5).

Table 13 – RMSE and *r* for green façade and roof, Atlântico Blue Studio

	13rd to 19th of February		27th of February to 13rd of March		18th of June to 2nd of July		5th to 10th of July	
	RMSE	Corre. (0-1)	RMSE	Corre. (0-1)	RMSE	Corre. (0-1)	RMSE	Corre. (0-1)
$T_{s.ext\ Zone\ 1}$ (°C)	2,310	0,834	3,569	0,823	2,424	0,930	1,803	0,918
$T_{s.ext\ Zone\ 2}$ (°C)	2,372	0,829	3,301	0,821	2,408	0,701	2,937	0,878
$T_{s.ext\ roof}$ (°C)	2,813	0,863	4,178	0,820	2,931	0,906	4,217	0,932

In Figure (13) is displayed the comparison between simulation and measured data collected by Prazeres (2015) for Zone 1 in green façade in July for Atlântico Blue Studio.

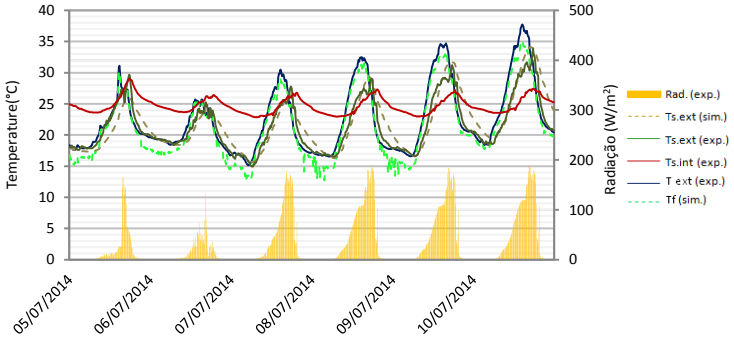

Figure 13: Comparison between simulation and measured data collected by Prazeres (2015), July, green façade, Atlântico Blue Studio

6.2.1 Malys et al. (2014) model

In Malys et al. (2014) model it was used the same inputs and outputs presented in chapter (4). The LAI and plant dimension was the same used in Table (11), and also the specific heat and wall density of Table (12). The RMSE was < 2°C for green wall and <3°C for green roof, and also had a good correlation between experimental and simulated data for both. These values are presented in Table (13).

Table 13 – RMSE and *r* for Level 2, Atlântico Blue Studio

	13rd to 19th of February		27th of February to 13rd of March		18th of June to 2nd of July		5th to 10th of July	
	RMSE	Corre. (0-1)	RMSE	Corre. (0-1)	RMSE	Corre. (0-1)	RMSE	Corre. (0-1)
$T_{s.ext\ Zone\ 1}$ (°C)	1,070	0,948	1,440	0,947	1,887	0,907	1,867	0,961
$T_{s.ext\ Zone\ 2}$ (°C)	1,030	0,950	1,640	0,911	1,621	0,787	1,764	0,906
$T_{s.ext\ Roof}$ (°C)	2,757	0,875	2,666	0,925	2,483	0,898	2,981	0,900

In Figure (14) is 8showed the comparison between simulation and measured data collected by Prazeres (2015) for Zone 1 of green façade in July for Atlântico Blue Studio.

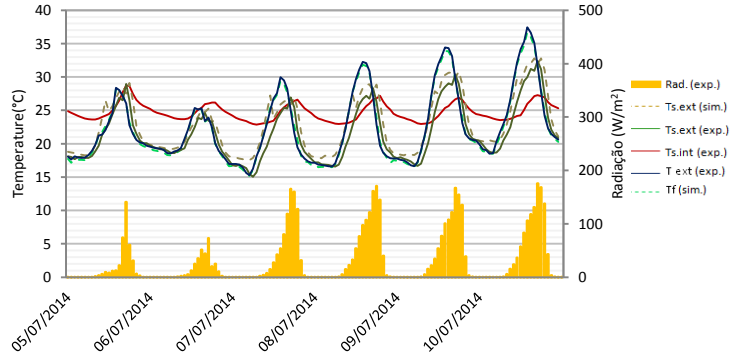

Figure 14: Comparison between simulation and measured data collected by Prazeres (2015), July, green façade, Atlântico Blue Studio

The green façade (Zone 1) outer surface temperature comparison between Susorova et al. (2013), Malys et al.

(2014) and the experimental collected by Prazeres (2015) is displayed in Figure (15).

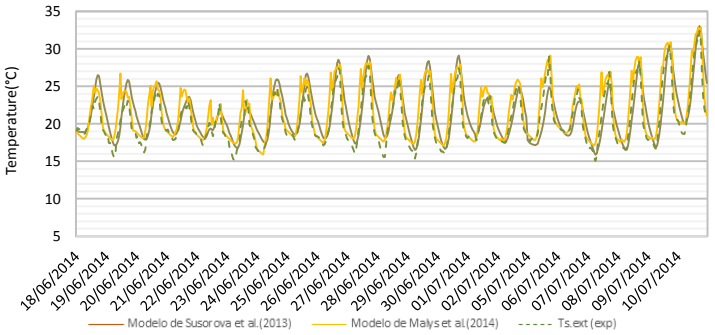

Figure 15: Comparison between simulation and measured data collected by Prazeres (2015), June, green façade, Atlântico Blue Studio

The biggest differences between the models appeared on 1st and 3rd March (5.23°C and 5.55°C). In June and July it was found that in Susorova et al. (2013) model the simulated outer surface temperature was closer to the experimental after the daily peak.

7. Conclusion and discussion

It is therefore concluded that Malys et al. (2014) model simulated better both study cases by presenting minor RMSE and better correlation with experimental simulated values.

In Travessa do Patrocínio was concluded that in February and March, the outer surface temperatures in Level 0 (no vegetation) were lower than the 2nd Floor (with vegetation), while in June and July didn't occurred. The outer surface temperature, between Level 0 and Level 2, oscillated 0.5°C to 8,1°C in winter, while in summer campaign oscillated 1.5°C to 8,4°C. The reasons for such events were due to the presence of vegetation on the facade. The plants provided the building less heat loss to the outside on the coldest days, while in warmer weather protected the building from the incident solar radiation.

In Atlantic Blue Studio it was concluded that the outer surface temperature decreased with the increase of LAI and size of plants. These increases have provided a better insulation of outer surface. Regarding the green roof, it was found that the outer surface temperatures were significantly higher than those presented by the green façade- The reason for this difference is focused on the roof's most sun exposure.

In addition to the thermal performance of green facades in Mediterranean climate, are presented suggestions for upcoming investigations, create implementing procedures for systems of green facades on buildings; establish rules and regulations for the use of these systems in Portugal; conduct an economic balance covering the investment and maintenance costs (irrigation, equipment, gardeners, etc.) of green facades in Portugal.

References

Alexandri, Elefheria e Jones, Phil. 2008. Temperature decreases in an urban canyon due to green walls and green roofs in diverse climates. *Building and Environment 43.* 2008, pp. 480-493.

Cameron, Ross W.F., Taylor, Jane E. e Emmett, Martin R. 2014. What´s cool in the world of green façades? How plant choice influences the cooling properties of green walls. *Building and Environment.* 2014, Vols. 73:198-207.

Eumorfopoulou, E.A. e Kontoleon, K.J. 2009. Experimental approach to the contribution of plant-covered walls to the thermal behaviour of building envelopes. *Building and Environment.* 2009, Vols. 44:1024-1038.

Eumorfopoulou, E.A. e Kontoleon, K.J.. 2010. The effect of the orientation and proportion of a plant-covered Wall layer on the thermal performance of a building zone. *Building and Environment 45.* 2010, pp. 1287-1303.

EnergyPlus Engineering Reference (2013) – Ernest Orlando Lawrence Berkeley National Laboratory, US Department of Energy, EUA.

Ismail, Mostafa. 2013. Quiet environment: Acoustics of vertical green wall systems of the Islamic urban form. *Frontiers of Architectural Research.* 2013, Vols. 2:162-177.

Köhler, M. e Bartfelder, F. 1987. Experimentelle untersuchungen zur function von fassadenbegrünungen. *Dissertação de Mestrado. Berlim 612S.* 1987.

Köhler, Manfred. 2008. Green Facades - A view back and some visions. *Urban Ecosyst.* Dezembro de 2008, pp. 11:423-36.

Malys, Laurent, Musy, Marjorie e Inard, Christian. 2014. A hydrothermal model to assess the impact of green walls on urban microclimate and building energy consumption. *Building and Environment 73.* 2014, pp. 187-197.

Ottelé, Marc, et al. 2011. Comparative life cycle analysis for green façades and living Wall systems. *Energy and Buildings.* 2011, Vols. 43:3419-3429, pp. 3419-3429.

Pérez, G., et al. 2011. Behaviour of green façades in Mediterranean Continental climate. *Energy Conversion and Management.* 2011, Vols. 52:1861-1867.

Perini, Katia e Rosasco, Paolo. 2013. Cost-benefit analysis for green façades and living wall systems. *Building and Environment.* 2013, Vols. 70:110-121.

Prazeres, Rita. 2015. Dissertação no Instituto Superior Técnico, "Monitorização de Fachadas Verdes".

Sheweka, Dr.Samar Mohamed e Mohamed, Arch. Nourhan Magdy. 2012. Green Façades as a New Sustainable Approach Towards Climate Change. *Energy Procedia.* 2012, Vols. 18:507-520.

Susorova, Irina, et al. 2013. A model of vegetated exterior facades for evaluation of wall thermal performance. *Building and Environment.* 2013, Vols. 67:1-13.

Wong, Nyuk Hien, et al. 2010. Thermal evaluation of vertical greenery systems for building walls. *Building and Environment.* 2010, Vols. 45:663-672.